Hindawi Publishing Corporation
International Journal of Polymer Science
Volume 2016, Article ID 2396817, 8 pages
http://dx.doi.org/10.1155/2016/2396817

Research Article

Upgrading Electrical, Mechanical, and Chemical Properties of CNTs/Polybond® Nanocomposites: Pursuit of Electroconductive Structural Polymer Nanocomplexes

Muhammad Sarfraz

Department of Polymer and Process Engineering, University of Engineering and Technology, Lahore, Pakistan

Correspondence should be addressed to Muhammad Sarfraz; msarfraz@uet.edu.pk

Received 20 June 2016; Revised 21 September 2016; Accepted 5 October 2016

Academic Editor: Cornelia Vasile

Electroconductive structural polymer-based nanocomposites (NCs) were prepared by incorporating carbon nanotubes (CNTs) into Polybond (PB) matrix via melt compounding technique. Chemical structure of NCs, investigated via Fourier transform infrared (FTIR) spectroscopy, corroborated successful grafting of CNTs functional groups onto PB chains. The morphology of NCs, as examined by scanning electron microscopy (SEM), ensured their optimum state of dispersion. Electrical conductivity, melting transition temperatures, mechanical properties, and chemical resistance of NCs were improved by incorporating CNTs into PB as established by differential scanning calorimetry (DSC), thermogravimetric analysis (TGA), high resistance meter (HRM), Universal Testing Machine (UTM), and chemical resistivity measurements, respectively.

1. Introduction

A carbon nanotube (CNT) is an allotrope of carbon arranged in the form of long cylindrical tube at nanoscale. CNTs, on the average, are several microns longer and have diameters in the range of 1–50 nm, and their typical length-to-diameter ratios are up to 10^8 [1]. Depending on their size, shape, thickness, number of structural layers, and type of helicity, CNTs may be classified as single-walled, multiwalled, nanobuds, nanofibers, and so forth. Owing to their extraordinary thermal, electrical, optical, and mechanical properties, CNTs find important applications in electronics, nanotechnology, optics, membranes, and other fields of materials science and technology as valuable additives [2].

In the recent decades, CNTs have been intensely considered as ideal reinforcing fillers for polymer nanocomposites on account of their high aspect ratio and good mechanical, electrical, and thermal properties [3–8]. These characteristic features suggest the improvement of mechanical [9], electrical [10], morphological, and thermal [11] properties of the base polymer by adding small quantities of CNTs. In addition, CNTs/polymer nanocomposites combine easy processability of polymers with excellent mechanical, electrical, and other valuable properties of CNTs.

Despite numerous studies in the field of polymer nanocomposites, full advantages of adding CNTs to polymer composites have not hitherto been fully utilized and few challenges pertaining to their fine dispersion and good interfacial adhesion within the polymer matrix need to be considered. Homogeneous dispersion and good adhesion at filler-polymer interface are considered to be important aspects to improve the properties of CNTs/polymer nanocomposites. Fine dispersion of CNTs is a key parameter to facilitate the appropriate distribution of the applied stress evenly between carbon nanotube bundles and to reduce stress concentrators. In addition, efficient interfacial adhesion is essential to conduct electricity and heat as well as to transfer stress from polymer matrix to the nanotubes [4, 12]. The strong van der Waals forces among the CNTs molecules, coupled with their high aspect ratio and surface area, usually lead to considerable agglomeration and poor deliverance of their superior properties to the matrix [13]. In consequence, homogeneous distribution of CNTs in polymer matrices imparts superior properties to the CNTs/polymer nanocomposites [14]. The

agglomeration of CNTs formed during their synthesis and van der Waals forces between CNTs should be minimized to homogeneously disperse CNTs into the polymers.

CNTs disperse well in polar polymers like polycarbonate [15], poly(methyl methacrylate) [16], poly(vinyl alcohol) [17], and polyacrylonitrile [18]. However, it is a challenge to disperse CNTs in apolar polymers, for example, polypropylene (PP) and polyethylene (PE), during melt processing. Various techniques like shear mixing [4, 12], end-group functionalization [19–21], plasma coating [22], and use of ionic surfactants [23] have been utilized to homogeneously distribute CNTs in PP matrix.

Homogeneous dispersion of CNTs into nonpolar polymers can be facilitated by adding a suitable compatibilizer to the system [15, 24–26]. PP and PE, two important nonpolar polymers, find applications in packaging, medical, construction, and automotive industries. CNTs are partially compatible with pure polymers resulting in poor dispersion and low quality materials [26–28]. These shortcomings can be overcome by functionalizing the polymer with grafting agents like acrylic esters, acrylic acid, and maleic anhydride [29, 30]. In this way, electrical and thermal properties of CNTs/polymer nanocomposites have been improved [12, 31–33]. Grafting agents containing maleic anhydride are helpful in refining the properties of composites. The interaction between amine or carboxyl groups of CNTs and functional groups grafted to polymer chains has helped to control the morphology and consolidated the interfacial adhesion between CNTs and polymer matrix [34].

Polybond 3000, chemically modified polypropylene grafted with 1.2 wt.% maleic anhydride as coupling agent, is one of the most promising candidates that can improve the properties of CNTs/PB nanocomposites. Polybond 3000 has not been reported so far and is a good choice for developing nanocomposites owing to its high level of functionality or chemical affinity for CNTs coupled with its low viscosity for excellent dispersion of the nanofiller. Depending on the chemical nature of Polybond 3000 matrix and CNTs nanofiller, the homogeneous dispersion of CNTs in PB matrix at nanoscale can be attained by forming a strong hydrogen bonding between maleic anhydride groups of PB and hydroxyl groups of CNTs. Incorporation of CNTs into compatibilized polymer can result in an increase of the molecular weight of the nanocomposite system thus improving the electrical and mechanical properties of the final nanocomposite. It is important to determine optimum loading of CNTs in the nanocomposite to enhance the dispersion without degrading its properties. The objective of this study is to prepare CNTs/Polybond nanocomposites (CNT/PB NC) in an attempt to improve their structural, thermal, electrical, and mechanical properties.

2. Experimental

2.1. Materials. Commercially available acid purified CNTs, synthesized via chemical vapor deposition method, were obtained from Cnano Technology. The polymer matrix Polybond 3000 having melt flow index 400 g/10 min, melting point 165°C, and specific gravity 0.91 was obtained from Special Chemtura. All the chemicals were used as received without further treatment.

2.2. Blending of CNTs/PB Nanocomposites. Polybond having 0, 0.5, 1, 2, 4, and 8 weight percent CNTs was blended in a Brabender mixer operating at 170°C for 15 minutes by setting the speed at 50 rpm. To avoid its sticking to mixer blades, the blend was removed from the mixer while still hot.

2.3. Preparation of Testing Specimens. The lumps of blended material were crushed down to use them in a hydraulic press. Hydraulic thermal press at 190°C under 200 MPa pressure was used to produce specimen sheets of varying thickness and diameter, subsequently to be used in various characterization processes. A template or die of specific shape can be used to mold the material as per requirement for a particular testing or characterization equipment.

2.4. Spectroscopic Analysis. Infrared spectra of absorption, emission, photoconductivity, and so forth of the samples were registered using JASCO FT/IR-4100 Infrared Spectrometer. It can be used for detecting various elements and functional groups in the nanocomposite specimen. The spectra of all the samples were recorded using potassium bromide (KBr) as an inert background material. The analysis was carried out in the frequency region of 500–4000 cm^{-1} with a resolution of 4 cm^{-1}.

2.5. Morphological Characterization. Scanning electron microscopic (SEM) images were taken to explore the morphology of CNTs/PB nanocomposites having different compositions by Hitachi S-4300SE/N SEM instrument. Testing specimens were cryofractured in liquid nitrogen followed by covering the outer surfaces with a thin gold film to avoid charging of electrons. The SEM microscope was operated at an accelerating voltage of 20 kV.

2.6. Thermal Properties. Glass transition (T_g) and melting (T_m) temperatures of CNTs/PB nanocomposite specimens were determined by differential scanning calorimetry (DSC) with a Netzsch DSC 200F3 calorimeter in the temperature range of 40–200°C at a heating rate of 5°C/min, under a nitrogen atmosphere with a flow rate of 50 mL/min. Thermal gravimetric analyses were conducted using a TGA/SDTA 851 (Mettler Toledo) system in air by heating from 100 to 700°C at a rate of 5°C min^{-1}.

2.7. Electrical Properties. Two-probe technique was used to determine electrical volume resistivity of the nanocomposites using Keithley 6517A electrometer (high resistance meter) and 8009 resistivity fixture. Compression molded sheets having dimensions of 100 × 100 mm were prepared using hydrodynamic thermal press by applying high pressure at a temperature of 190°C and then cut into square shaped specimens. The thickness of the film was measured using SEM. Following the standards of ASTM D-257, the specimens were subjected to a constant voltage of 50 V and a current of 1 mA under ambient conditions.

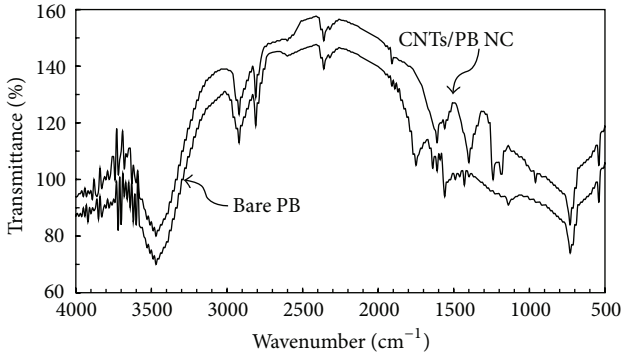

Figure 1: FT-IR spectra of base Polybond and one of the representative samples of CNTs/PB nanocomposites.

2.8. Mechanical Testing. The specimens for the mechanical testing were prepared using a hydraulic compression molding machine (Gibitre®, Italy) at 190°C. Static tensile testing was performed on TIRA Test 2810 Universal Testing Machine (UTM) at room temperature according to ASTM D638. Izod pendulum impact strength was determined using a Falling Dart Impact Tester (FDIT) according to the standards of ASTM D2794 using an indenter weighing 1.8 kg at 23°C. Sample thickness was varied in the range of 0.4–0.8 mm.

2.9. Water Absorption. Water absorption test was accomplished by following the standards of ASTM D570. The tests were carried out at room (25°C) and elevated (80°C) temperatures by submerging the test specimens in distilled water for a particular period of time. The testing specimen was compression molded in the form of 50.8 mm diameter and 3.2 mm thick disk, weighed, and immersed in distilled water at 25°C. The specimen was taken out of water beaker after 24 hours; water from outer surfaces was wiped off with a dry fabric and again weighed with an accuracy of nearest 1 mg. The same procedure was replicated to measure water absorption at 80°C.

3. Results and Discussions

3.1. Fourier Transform Infrared Spectroscopy. FTIR spectra recorded for unfilled Polybond 3000 and one of the representative specimens of CNTs/PB nanocomposites, with the assigned peak positions, are shown in Figure 1.

The IR absorption peaks appearing at 720 and 1715 cm^{-1} correspond to the C-H out-of-plane deformation of MA and the carboxylic acid, respectively. The appearance of absorption band at 1168 cm^{-1} is associated with -CH_3 group. The normalized peaks appearing, respectively, at 888 cm^{-1} (associated with vinylidene) and 1648 cm^{-1} (associated with stretching of double bonds) maintain chain-scission. The characteristic absorption band at 1792 cm^{-1} is correlated with the broadening of symmetric C=O bond of anhydride functional groups grafted to PB. The absorption peaks appearing at 1,140 and 1,750 cm^{-1} are, respectively, related to the stretching vibration modes of C-O and C=O. Furthermore, the absorption peaks at 1,560 and 1,430 cm^{-1} correspond to stretching of carboxylate ions. The peaks displayed at 1,560 and 1,750 cm^{-1} indicate the presence of carboxyl groups which can play a vital role in reacting with maleic anhydride thus controlling the interfacial adhesion between PB and CNTs.

For the identification of functional groups connected to CNTs surfaces, the representative FTIR spectra of CNTs/PB nanocomposites along with noticeable peak positions are shown in Figure 1. The structural modification of CNTs due to carboxylation (representative of C=C group) is indicated by absorption bands shift from 1600 cm^{-1} to 1235 and 1400 cm^{-1}. A distinct band originated at 1659 cm^{-1} can be attributed to an antisymmetric stretch of C-O group. The infrared peak appearing at 1740 cm^{-1} corresponds to the stretching mode of carbonyl (C=O) group. The absorption bands that appeared at 2950 and 3450 cm^{-1}, respectively, are characteristics of stretching vibrations of C-H and O-H groups.

3.2. Morphological Characterization. SEM was used to analyze the surface morphology and tropology of the nanocomposite specimens at nanoscale. The extent of distribution of nanofiller within the polymer matrix mainly determines the performance of nanofilled-polymer nanocomposites. Hence, the morphological characterization of nanocomposites is especially a key parameter to assess the proper distribution of CNTs in the polymer matrix.

In this study, scattering of CNTs in CNTs/PB nanocomposites was examined by SEM (Figure 2). The selected SEM observations are representative of the distribution of CNTs in the Polybond matrix. A small number of carbon nanotubes were detected on the nanocomposite surface indicating even dispersion and distribution of nanotubes along with formation of minute aggregates.

To determine the effect of concentration of CNTs on their dispersion within the PB matrix, nanocomposite surfaces were examined by SEM. For their low weight fractions (0.5–1 wt.%), the dispersion of CNTs was uniform and there was no agglomeration (Figures 2(b)-2(c)). A relatively good homogenous dispersion of CNTs was observed for moderately filled (2–4 wt.%) nanocomposites (Figures 2(d)-2(e)). With the further addition of CNTs, indications of slight aggregation of CNTs can be observed for higher loading (e.g., 8 wt.%) of CNTs as depicted in Figure 2(f). These results are in parallel with and reflect the findings of the electrical resistivity.

3.3. Thermal Properties. In order to study their phase transitions, thermal stability, and physical and chemical phenomena, DSC and TGA-DTG analyses of all the materials were carried out in the range of 100–700°C as outlined in Table 1. TGA measurements up to 700°C were carried out to thoroughly examine the thermal behavior of nanocomposites. Addition of CNTs to Polybond improved its characteristic thermal parameters as a function of CNTs content as indicated in Figures 3 and 4.

The improvement in rigidity of nanocomposites, as measured in terms of T_g or T_m, with increasing CNTs contents can be correlated to the restricted movement of polymer chains

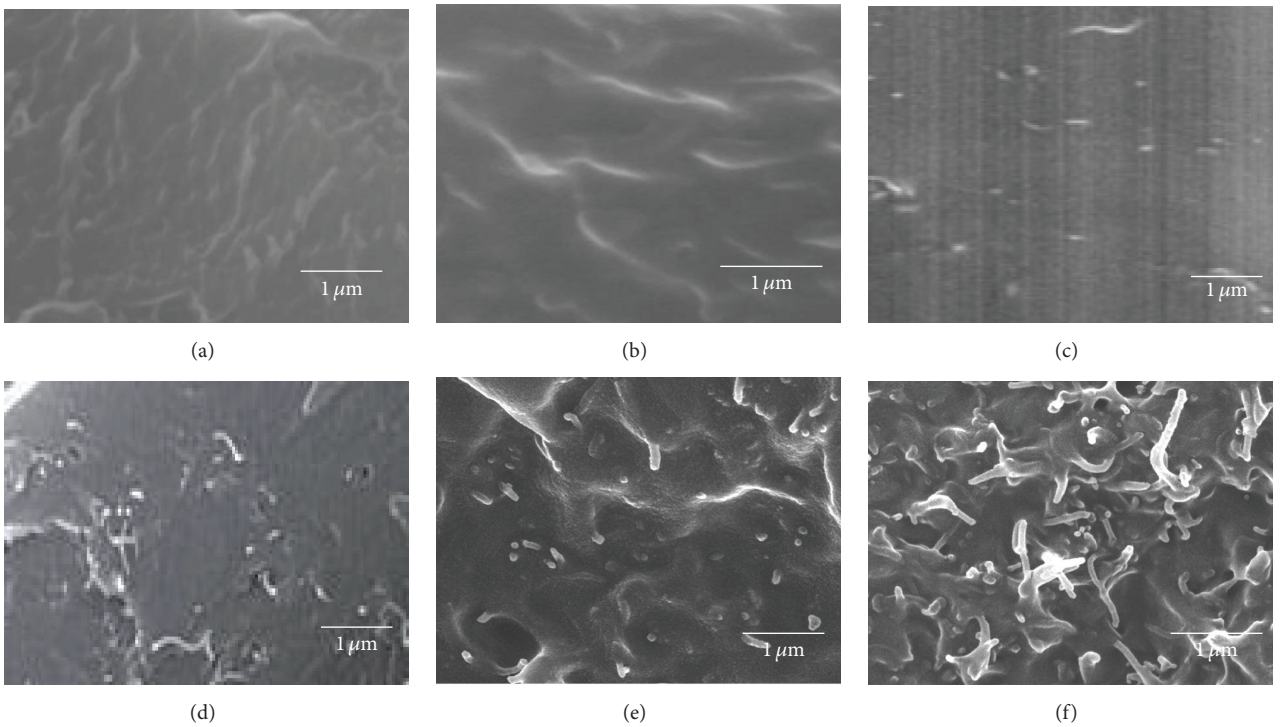

Figure 2: High resolution cross-sectional scanning electron micrographs of unfilled PB (a) and CNTs/PB nanocomposites filled with 0.5 (b), 1 (c), 2 (d), 4 (e), and 8 (f) wt.% CNTs.

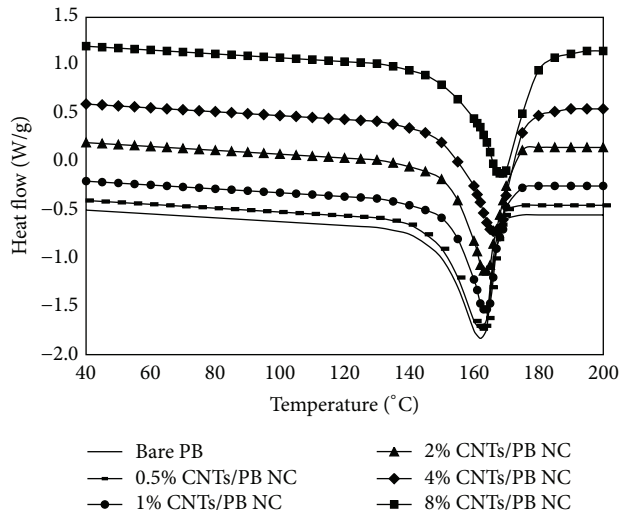

Figure 3: DSC curves of unfilled PB and CNTs/PB nanocomposites containing 0.5, 1, 2, 4, and 8 wt.% CNTs.

Table 1: Characteristic temperatures, peaks, and residual masses of nanocomposites acquired from TGA-DTG data.

Sample designation	T_g (°C)	T_m (°C)	$T_{d5\%}$ (°C)	$T_{d10\%}$ (°C)	DTG peak (°C)	Residual mass (%)
Bare PB	177	163	420	438	468	0.7
0.5% CNTs/PB NC	181	163.4	419	438	468	0.99
1% CNTs/PB NC	182	163.7	418	437	469	1.1
2% CNTs/PB NC	184	163.9	416	436	470	1.7
4% CNTs/PB NC	188	164.6	414	434	472	2.1
8% CNTs/PB NC	190	165.7	412	432	474	2.8

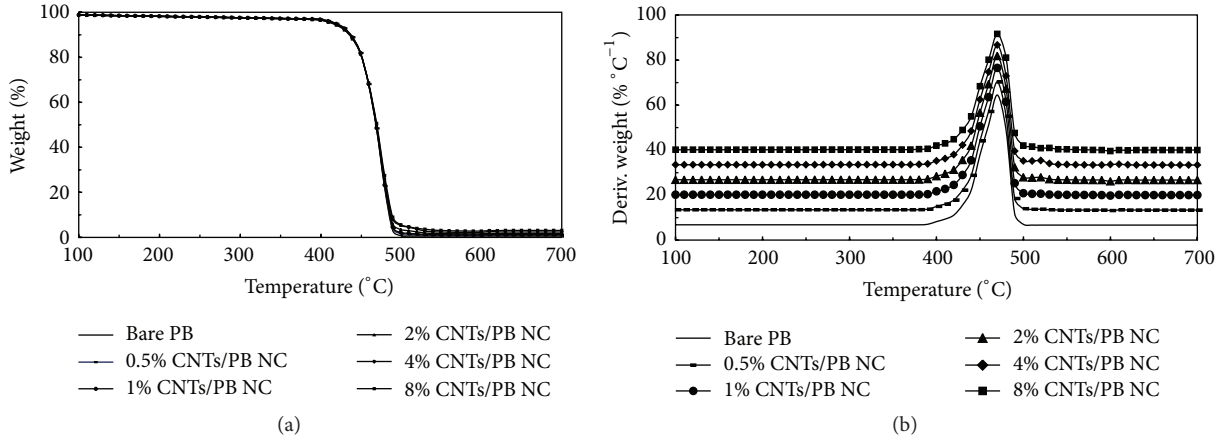

Figure 4: TGA-DTG curves: TGA (a) and DTG (b) of unfilled PB and CNTs/PB nanocomposites containing 0.5, 1, 2, 4, and 8% by weight of CNTs.

owing to mutual interactions occurring among polymer chains and CNTs (Figure 3). This can be associated with the higher heat resistance of the dispersed nanofiller phase as compared to that of the continuous polymer matrix.

The TGA curves of all the prepared samples indicate one prominent weight loss curve corresponding to pyrolysis (390–500°C) as shown in Figure 4(a). The weight loss during this step can be attributed to degradation of PB chains along with the decomposition of organic components of CNTs. The residual weight at the end of analyses helped to verify nominal mass contents of added CNTs in corresponding samples.

The temperatures at which testing specimen loses its 5 and 10 percent weight, denoted by $T_{d5\%}$ and $T_{d10\%}$, respectively, in TGA analysis determine the thermal stability of a material [35]. Table 1 summarizes some important thermal parameters of the synthesized materials. Values of $T_{d5\%}$ and $T_{d10\%}$ occur between 412–420°C and 433–438°C, respectively, with both parameters being decreasing function of CNTs contents. The DTG curves illustrated in Figure 4(b) also give information on pyrolysis rates; the residual masses of all the materials are enlisted in Table 1.

As indicated by weight loss curves, the thermal stability of nanocomposites, determined in terms of DTG peaks, improved with increasing CNTs contents. Since the maximum temperature experienced in different applications using electroconducting structural materials falls in the range of 30 to 350°C, these nanocomposites can safely be used in the relevant applications.

3.4. Electrical Properties. The electrical conductivity of pure polymer drastically increased due to the addition of highly conducting carbon nanotubes. The electrical properties of low CNTs-filled polymer nanocomposites (0.1–2 wt.%) turn into semiconducting materials and can be further improved if moderately filled (2–5 wt.%) with CNTs as shown in Figure 5. The volume resistivity of CNTs/PB nanocomposites as a function of CNTs weight fraction is also displayed in Figure 5.

Possessing good electrical properties, incorporation of CNTs into nonconducting polymers is found to be significant

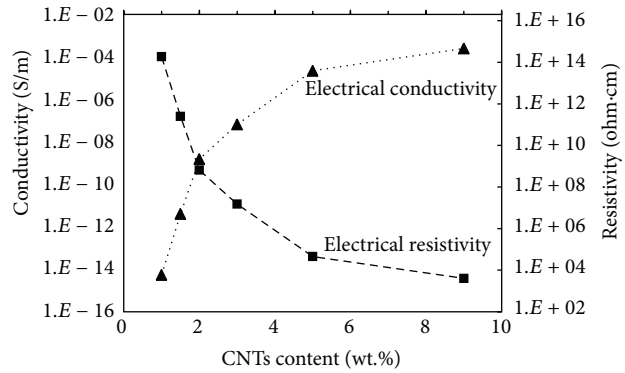

Figure 5: Variation of electrical resistivity and conductivity with increase in CNTs contents.

in enhancing the electrical conductivity of nanocomposites. The concentration of CNTs at which conductivity of nanocomposites increases sharply is generally termed as electrical percolation threshold. At this specific concentration, CNTs form a three-dimensional network throughout the polymer chains thus generating a conducting path within the nanocomposite framework. This value strongly depends on the alignment, aspect ratio, and degree of surface modification of CNTs, coupled with homogeneous distribution and suitable interfacial interaction of CNTs and PB matrix. The formation of percolation path of CNTs, in the low range of nanofiller concentration (0.1–1 wt.%), can lead to greatly improved electrical conductivity of the unfilled polymer.

The nanocomposite demonstrated a sudden decrease in resistivity at 4 wt.% loading of CNTs, thus signifying the development of percolation network. The phenomenon of percolation can be better understood in terms of the formation of additional electrical pathways among CNTs during the nanocomposite development while in molten state. It can be attributed to the improved dispersion of CNTs owing to their specific interaction with polymer chains. Beyond the percolation threshold concentration, there is nominal decrease in electrical resistivity of the specimen

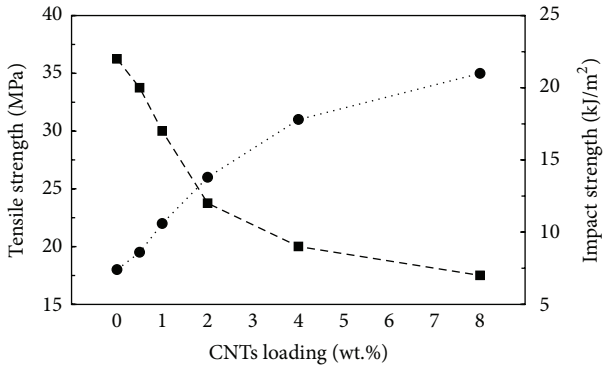

Figure 6: Tensile strength and impact strength of nanocomposites acquired, respectively, from static stress-strain and Izod pendulum impact testing data.

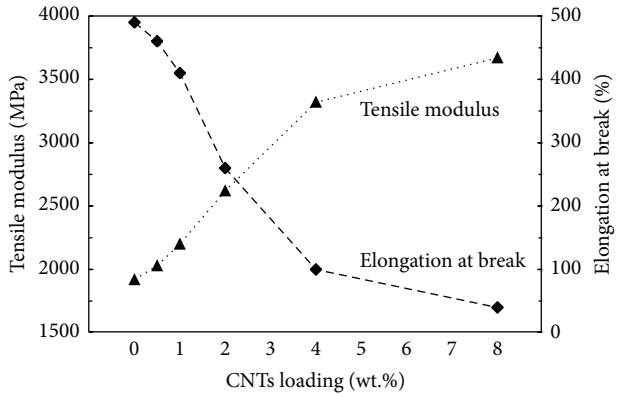

Figure 7: Tensile modulus and elongation at break of nanocomposites determined from static stress-strain testing data.

since few further conduction paths are generated owing to slight agglomeration of CNTs.

3.5. Mechanical Properties. The mechanical properties of samples were measured using UTM and TIT. The specimens were prepared in a template using hydraulic press and the mechanical tests were performed to measure tensile strength, elongation at break, tensile modulus, and Izod impact strength. The advantages of blending are also demonstrated by the mechanical properties of the nanocomposites.

The parameters obtained from static stress-strain and Izod impact testing are represented in Figures 6 and 7, respectively. The base PB has amorphous structure that results in a flexible material as indicated by high value of elongation-to-break. The maximum tensile strength of the specimens has increased from 17 MPa (for base Polybond) to much higher values of 35 MPa (for CNTs/PB nanocomposite containing 8 wt.% CNTs contents). Similarly, the impact strength of CNTs/PB nanocomposite has increased significantly as compared to unfilled PB showing improvement in toughness of the material by blending.

For high level of maximum stress values, CNTs/PB nanocomposite with the highest content (i.e., 8% CNT by weight) shows the highest ultimate elongation (Figure 7) along with

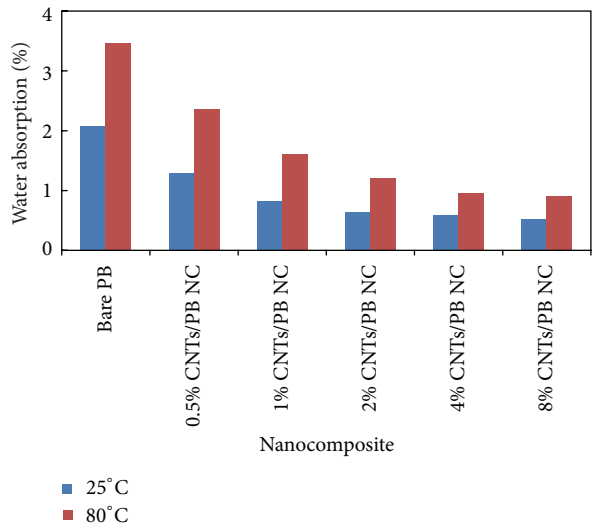

Figure 8: Water absorption data of bare PB and CNTs/PB nanocomposites determined at ambient (25°C) and elevated (80°C) temperatures.

the highest modulus value. This can be attributed to the formation of networking structure of the CNTs for high levels of grafting that resulted in much improved mechanical properties. The same effects can also be confirmed by the high values of the impact strength of the CNTs/PB nanocomposite.

3.6. Water Absorption Testing. The water absorption properties play a vital role if the material is susceptible to encountering wet or misty environmental conditions. The specimen material was conditioned by keeping it in an oven at 100°C for an hour to ensure its complete dehydration. The conditioned specimen was weighed and then immersed in demineralized water in a beaker, both at ambient (25°C) and elevated (80°C) temperatures, for 24 hours.

The blended nanocomposite samples show lower water absorption as compared to base Polybond as reported in Figure 8. The higher the CNTs contents in the nanocomposite, the lower the level of water absorption at a given temperature on account of higher degree of networking/grafting of the material due to addition of CNTs. However, at higher temperatures (e.g., 80°C as compared to 25°C in this case), the water intake of the nanocomposites increases owing to polymer chain swelling and increased void volume.

4. Conclusions

The effect of varying CNTs loadings on characteristic properties of CNTs/Polybond 3000 nanocomposites was investigated. Morphological characterization based on scanning electron microscopy revealed that CNTs are homogeneously dispersed in the polymer matrix thus resulting in improved filler-polymer interfacial adhesion. Thermal stability and glass transition temperature of prepared nanocomposites were improved by incorporation of CNTs. Addition of CNTs contents drastically improved the electrical conductivity of the bare polymer. The mechanical characterization has shown

that both tensile modulus and strength of nanocomposites greatly increased by many orders of magnitude due to addition of CNTs. An issue, which needs to be further investigated, is that tensile elongation at break decreases with the addition of CNTs. With the addition of CNTs, water absorption capacity of the nanocomposites decreases thus making them suitable under humid conditions.

Competing Interests

The author declares that they have no competing interests.

Acknowledgments

The author is thankful to Department of Chemical Engineering, King Fahd University of Petroleum and Minerals, Dhahran, Kingdom of Saudi Arabia, for providing laboratory facilities for this work.

References

[1] X. Wang, Q. Li, J. Xie et al., "Fabrication of ultralong and electrically uniform single-walled carbon nanotubes on clean substrates," *Nano Letters*, vol. 9, no. 9, pp. 3137–3141, 2009.

[2] S. Gullapalli and M. S. Wong, "Nanotechnology: a guide to. Nano-objects," *Chemical Engineering Progress*, vol. 107, p. 5, 2011.

[3] M.-K. Seo, J.-R. Lee, and S.-J. Park, "Crystallization kinetics and interfacial behaviors of polypropylene composites reinforced with multi-walled carbon nanotubes," *Materials Science and Engineering A*, vol. 404, no. 1-2, pp. 79–84, 2005.

[4] Y. Xiao, X. Zhang, W. Cao et al., "Dispersion and mechanical properties of polypropylene/multiwall carbon nanotubes composites obtained via dynamic packing injection molding," *Journal of Applied Polymer Science*, vol. 104, no. 3, pp. 1880–1886, 2007.

[5] Z. Jin, K. P. Pramoda, G. Xu, and S. H. Goh, "Dynamic mechanical behavior of melt-processed multi-walled carbon nanotube/poly(methyl methacrylate) composites," *Chemical Physics Letters*, vol. 337, no. 1–3, pp. 43–47, 2001.

[6] W. K. Park, J. H. Kim, S. S. Lee, J. Kim, G. W. Lee, and M. Park, "Effect of carbon nanotube pre-treatment on dispersion and electrical properties of melt mixed multi-walled carbon nanotubes / poly(methyl methacrylate) composites," *Macromolecular Research*, vol. 13, no. 3, pp. 206–211, 2005.

[7] G. D. Liang and S. C. Tjong, "Electrical properties of low-density polyethylene/multiwalled carbon nanotube nanocomposites," *Materials Chemistry and Physics*, vol. 100, no. 1, pp. 132–137, 2006.

[8] K. Mylvaganam and L. C. Zhang, "Fabrication and application of polymer composites comprising carbon nanotubes," *Recent Patents on Nanotechnology*, vol. 1, no. 1, pp. 59–65, 2007.

[9] M. Ganß, B. K. Satapathy, M. Thunga, R. Weidisch, P. Pötschke, and D. Jehnichen, "Structural interpretations of deformation and fracture behavior of polypropylene/multi-walled carbon nanotube composites," *Acta Materialia*, vol. 56, no. 10, pp. 2247–2261, 2008.

[10] O. Valentino, M. Sarno, N. G. Rainone et al., "Influence of the polymer structure and nanotube concentration on the conductivity and rheological properties of polyethylene/CNT composites," *Physica E: Low-Dimensional Systems and Nanostructures*, vol. 40, no. 7, pp. 2440–2445, 2008.

[11] D. Bikiaris, A. Vassiliou, K. Chrissafis, K. M. Paraskevopoulos, A. Jannakoudakis, and A. Docoslis, "Effect of acid treated multi-walled carbon nanotubes on the mechanical, permeability, thermal properties and thermo-oxidative stability of isotactic polypropylene," *Polymer Degradation and Stability*, vol. 93, no. 5, pp. 952–967, 2008.

[12] M. A. L. Manchado, L. Valentini, J. Biagiotti, and J. M. Kenny, "Thermal and mechanical properties of single-walled carbon nanotubes-polypropylene composites prepared by melt processing," *Carbon*, vol. 43, no. 7, pp. 1499–1505, 2005.

[13] D. Qian, E. C. Dickey, R. Andrews, and T. Rantell, "Load transfer and deformation mechanisms in carbon nanotube-polystyrene composites," *Applied Physics Letters*, vol. 76, no. 20, pp. 2868–2870, 2000.

[14] L. Jin, C. Bower, and O. Zhou, "Alignment of carbon nanotubes in a polymer matrix by mechanical stretching," *Applied Physics Letters*, vol. 73, no. 9, pp. 1197–1199, 1998.

[15] L. Chen, X.-J. Pang, and Z.-L. Yu, "Study on polycarbonate/multi-walled carbon nanotubes composite produced by melt processing," *Materials Science and Engineering A*, vol. 457, no. 1-2, pp. 287–291, 2007.

[16] J. Zeng, B. Saltysiak, W. S. Johnson, D. A. Schiraldi, and S. Kumar, "Processing and properties of poly(methyl methacrylate)/carbon nano fiber composites," *Composites Part B: Engineering*, vol. 35, no. 2, pp. 173–178, 2004.

[17] X. Zhang, T. Liu, T. V. Sreekumar, S. Kumar, X. Hu, and K. Smith, "Gel spinning of PVA/SWNT composite fiber," *Polymer*, vol. 45, no. 26, pp. 8801–8807, 2004.

[18] H. G. Chae, T. V. Sreekumar, T. Uchida, and S. Kumar, "A comparison of reinforcement efficiency of various types of carbon nanotubes in polyacrylonitrile fiber," *Polymer*, vol. 46, no. 24, pp. 10925–10935, 2005.

[19] D. McIntosh, V. N. Khabashesku, and E. V. Barrera, "Nanocomposite fiber systems processed from fluorinated single-walled carbon nanotubes and a polypropylene matrix," *Chemistry of Materials*, vol. 18, no. 19, pp. 4561–4569, 2006.

[20] D. McIntosh, V. N. Khabashesku, and E. V. Barrera, "Benzoyl peroxide initiated in situ functionalization, processing, and mechanical properties of single-walled carbon nanotube–polypropylene composite fibers," *The Journal of Physical Chemistry C*, vol. 111, no. 4, pp. 1592–1600, 2007.

[21] Z. Zhou, S. Wang, L. Lu, Y. Zhang, and Y. Zhang, "Isothermal crystallization kinetics of polypropylene with silane functionalized multi-walled carbon nanotubes," *Journal of Polymer Science, Part B: Polymer Physics*, vol. 45, no. 13, pp. 1616–1624, 2007.

[22] D. Shi, J. Lian, P. He et al., "Plasma coating of carbon nanofibers for enhanced dispersion and interfacial bonding in polymer composites," *Applied Physics Letters*, vol. 83, no. 25, pp. 5301–5303, 2003.

[23] L. Vaisman, G. Marom, and H. D. Wagner, "Dispersions of surface-modified carbon nanotubes in water-soluble and water-insoluble polymers," *Advanced Functional Materials*, vol. 16, no. 3, pp. 357–363, 2006.

[24] S. H. Jin, C. H. Kang, K. H. Yoon, D. S. Bang, and Y. B. Park, "Effect of compatibilizer on morphology, thermal, and rheological properties of polypropylene/functionalized multi-walled carbon nanotubes composite," *Journal of Applied Polymer Science*, vol. 111, pp. 1028–1033, 2009.

[25] S. H. Lee, M. W. Kim, S. H. Kim, and J. R. Youn, "Rheological and electrical properties of polypropylene/MWCNT composites prepared with MWCNT masterbatch chips," *European Polymer Journal*, vol. 44, no. 6, pp. 1620–1630, 2008.

[26] K. Prashantha, J. Soulestin, M. F. Lacrampe, M. Claes, G. Dupin, and P. Krawczak, "Multi-walled carbon nanotube filled polypropylene nanocomposites based on masterbatch route: Improvement of dispersion and mechanical properties through PP-g-MA addition," *Express Polymer Letters*, vol. 2, no. 10, pp. 735–745, 2008.

[27] D. Wu, Y. Sun, and M. Zhang, "Kinetics study on melt compounding of carbon nanotube/polypropylene nanocomposites," *Journal of Polymer Science, Part B: Polymer Physics*, vol. 47, no. 6, pp. 608–618, 2009.

[28] N. Hasegawa, M. Kawasumi, M. Kato, A. Usuki, and A. Okada, "Preparation and mechanical properties of polypropylene-clay hybrids using a maleic anhydride-modified polypropylene oligomer," *Journal of Applied Polymer Science*, vol. 67, no. 1, pp. 87–92, 1998.

[29] A. Kelarakis, K. Yoon, I. Sics et al., "Shear-induced orientation and structure development in isotactic polypropylene melt containing modified carbon nanofibers," *Journal of Macromolecular Science—Physics*, vol. 45, no. 2, pp. 247–261, 2006.

[30] X. P. Zhou, X. L. Xie, F. Zeng, R. K. Y. Li, and Y. W. Mai, "Properties of polypropylene/carbon nanotube composites compatibilized by maleic anhydride grafted SEBS," *Key Engineering Materials*, vol. 312, pp. 223–228, 2006.

[31] S. C. Tjong, G. D. Liang, and S. P. Bao, "Electrical behavior of polypropylene/multiwalled carbon nanotube nanocomposites with low percolation threshold," *Scripta Materialia*, vol. 57, no. 6, pp. 461–464, 2007.

[32] X. Jiang, Y. Bin, N. Kikyotani, and M. Matsuo, "Thermal, electrical and mechanical properties of ultra-high molecular weight polypropylene and carbon filler composites," *Polymer Journal*, vol. 38, no. 5, pp. 419–431, 2006.

[33] S. H. Lee, E. Cho, S. H. Jeon, and J. R. Youn, "Rheological and electrical properties of polypropylene composites containing functionalized multi-walled carbon nanotubes and compatibilizers," *Carbon*, vol. 45, no. 14, pp. 2810–2822, 2007.

[34] G.-W. Lee, S. Jagannathan, H. G. Chae, M. L. Minus, and S. Kumar, "Carbon nanotube dispersion and exfoliation in polypropylene and structure and properties of the resulting composites," *Polymer*, vol. 49, no. 7, pp. 1831–1840, 2008.

[35] Y. C. Xiao, T. S. Chung, H. M. Guan, and M. D. Guiver, "Synthesis, cross-linking and carbonization of co-polyimides containing internal acetylene units for gas separation," *Journal of Membrane Science*, vol. 302, no. 1-2, pp. 254–264, 2007.